OFFSHORE TECHNOLOGY CONFERENCE
6200 North Central Expressway
Dallas, Texas 75206

PAPER NUMBER OTC 2312

THIS PRESENTATION IS SUBJECT TO CORRECTION

Field Testing and Analysis of Laterally Loaded Piles in Stiff Clay

By

Lymon C. Reese, The U. of Texas, William R. Cox, TERA, Inc, and Francis D. Koop
Lawrence-Allison & Associates

Abstract

Two nominally 24-in. diameter piles, instrumented for measuring bending moments, were driven into stiff clay and subjected to lateral loading. A nominally 6-in. diameter pile was also instrumented for measuring bending moments. It was driven at the same site, loaded, pulled, redriven, and reloaded. Short-term static and cyclic loading was employed on both 24-in. diameter and 6-in. diameter piles. The water table was maintained a few inches above the ground surface during the testing program.

The results of the tests were analyzed to obtain families of curves showing soil resistance p as a function of pile deflection y. Based on the experimental p-y curves and on theory for the behavior of soil, procedures for predicting p-y curves for stiff clay were developed. The procedures were used and predictions of pile behavior at the site were made. The predictions compared favorably with actual behavior.

References and Illustrations at end of paper.

Foreword

The research described in this paper was sponsored by Amoco Production Company, Chevron Oil Field Research, Exxon Production Research Company, Mobil Oil Corporation, and Shell Development Company. Shell Development Company was the operator of the project.

Location of Test Site

The field studies on which this paper is based were made at a location five miles to the northeast of Austin, Texas adjacent to US Highway 290. The surface soils in this area consist of stiff, preconsolidated clays of marine origins. These clays are referred to as the Taylor group and studies showed that unconfined compressive strengths of 2 to 10 tons/sq ft were not uncommon in zones near the surface.

These clays have a secondary structure, such as fissures, joints or slickensides, that was desirable because of the wide occurrence of this type of soil in nature. The secondary structure was expected to result in a less favorable behavior of the clay; therefore, a possibly critical soil condition could be investigated.

Preparation of Test Site

On December 15, 1966, a pit 45 ft wide by 50 ft long by 3 ft deep was excavated at the test site. A plan of the test area is shown in Fig. 1

with the locations of all soil borings and test piles.

After the excavation was completed the pit was flooded with water to saturate the near surface clays and to simulate conditions that would exist in clays on the ocean floor. This initial inundation was done some five months before the installation of the first test piles and some six months before lateral loading of test piles.

In April 1967, two soil borings, borings 5 and 6, were made to investigate the influence of some four months of ponding on the water content of the clay. These borings indicated an increase in water content with an accompanying decrease in shear strength for clays in the first few feet below the pit bottom. After borings 5 and 6, the pit was lowered an additional 2-1/2 ft. This additional excavation was done on April 21, 1967 and the pit was again inundated.

Test piling and associated equipment were installed in the pit during the period from May 2 through May 9, 1967. During this period the water in the pit was removed but the clay was prevented from drying by local ponding. After all construction was completed, an additional 1/2 ft of soil was removed from the pit thus placing the bottom of the pit approximately 6 ft below original ground surface. The pit was again flooded and it remained inundated until all testing was completed.

Soil Investigations

A chronological list of the nine borings made at the site are as follows:

Borings	Date of Boring	Status of Test Program
B-1, B-2	10/14/66	Before excavating test pit.
B-3, B-4	12/15/66	After excavating pit to 3 ft depth and just prior to ponding.
B-5, B-6	4/12/67	After ponding for 4 months. Prior to installation of test piles in period of May 2-9, 1967.
B-7, B-8	6/30/67	Pit excavated another 2-1/2 ft to total depth of 5-1/2 ft on April 21, 1967. Test piles installed and pit excavated a final 1/2 ft to total depth of 6 ft in period May 2-9, 1967. First test pile loaded statically and cyclically in period June 12-21, 1967.
B-9	2/10/68	Tests made on soil samples obtained in 24-in. diameter holes augered during salvage operations of test piles.

Boring logs for borings 5 and 6 are given in Figs. 2 and 3. These two borings are representative of conditions found at the site. Undisturbed samples were taken with thin-walled steel sampling tubes with a 20 degree beveled cutting edge, a 3-in. O.D., and a 0.085 in. thick wall. The tubes were advanced by pushing.

Triaxial tests were unconsolidated-undrained with confining pressures conforming to in situ pressures. Failures observed in samples tested in compression in the laboratory were of three general types: (1) pure joint movements on slickensided surfaces, (2) shear through softer clay material which completely filled joints, and (3) bulge or shear which cut across any observed joints and apparently was unaffected by them. The first type was observed to be most prevalent of all and occurred in the middle depths. The second type was found mostly at greater depths. The third type was found in the shallow softer clays.

Representative stress-strain curves of soil samples are given in Fig. 4. A composite log based on borings 5 through 9 is given in Fig. 5.

Comments on the accuracy of shear strength given in the composite boring log are as follows:

(1) In the medium soft clays found in the upper 4 feet, referred to pit-bottom, the in situ shear strength is accurately represented in Fig. 5.

(2) In the zone from 4 to 10 feet, the effect of jointing is serious and the actual shear strength is less accurately known. It is believed to be less than indicated by the penetrometer (maximum capacity, 2.5 tons/sq ft), but more than indicated by the triaxial test.

(3) Below 10 feet, jointing is still important, but the triaxial test results are probably good indicators.

Test Piles

The 24-in. diameter test piles and other equipment had been used in a test program on laterally loaded piles in sand at Mustang Island, Texas (1,2). Discussion here will be limited to modifications of the piles and to a description of the fabrication of a 6-in. test pile.

For the tests in stiff clays it was necessary to increase the existing 3/8-in. wall thickness in the top 23 ft of each 24-in. diameter pile. This was accomplished by wrapping the pile with two 5/8-in. thick simicircular steel sections 23 ft in length. The 5/8-in. thick wrappers were attached by circumferential welds at the flange of the test pile and at the bottom of the wrapper section, and by two longitudinal welds.

The 6.625-in. diameter test pile was made up of an upper 28-ft long instrumented section and a 15-ft long uninstrumented lower section. The 28-ft and 15-ft sections had wall thicknesses of 0.718 in. and 0.375 in., respectively.

To allow the installation of strain gages in the 6-in. diameter pile, the pile length was cut into eight sections. Twenty metal-foil strain gages were installed in these sections by reaching inside the sections from each end. After the strain gages were installed, cable was strung and the sections were connected by circumferential welds. A 1-in.-thick diaphragm was welded at the bottom and at the top of the instrumented section in order to provide a sealed environment for the strain gages and cables.

Calibration of Test Piles

The two 24-in. piles were placed horizontally and connected at the ends with steel straps to create simple beam supports. They were then jacked apart by using a hydraulic ram and a load cell in series.

A total of six loading series was run on each 24-in. pile, three to relieve stress concentrations which may have developed because of the addition of the 5/8-in. thick wrappers and three for recording data. A maximum load of 50,000 lb was applied, which corresponded to a maximum stress of about 15,000 lb/sq in.

The 6-in. pile was connected to a 24-in. pile by tension straps and a scissors jack was placed between the piles to jack the piles apart. Loads applied to the piles were monitored by a 5000-lb proving ring placed along the loading axis of the scissors jack. A total of 12 loadings was run on the pile. The maximum applied load was 5000 lb, corresponding to a maximum stress in the pile wall of 20,000 lb/sq in.

Installation of Piling and Test Equipment

Each of the two 24-in. diameter test piles had a total length of 60 ft. The elevations of the pile during testing and the arrangement of testing equipment are indicated in Fig. 6.

An open ended 18-ft long bottom section of the 24-in. pile was driven with a Delmag D-12 diesel hammer. The inside of these sections were then cleaned out using a 23-in. diameter auger and holes were advanced to a depth of 48 ft using the same 23 in. auger.

The 32-ft instrumented sections were then welded to the 18-ft bottom sections and driving was resumed with the Delmag hammer until the flanges on the instrumented sections were one foot above the grade elevation of the test pit bottom. At this position, the test piles had a final penetration of 49 ft into the soil. The 24-in. diameter test piles were designated as piles 1 and 2.

The 6-in. diameter pile had a total length of 43 ft and was driven to a penetration of 29 ft into the soil. In the installation procedure, a 15-ft uninstrumented section was driven first. This section was augered out with a 5-1/2-in. diameter auger to a total depth of 29 ft. The 28-ft long instrumented section was then welded to the bottom section and driving was resumed to final penetration. A drawing of the test setup for the 6-in. diameter pile is given in Fig. 7.

The 6-in. diameter pile was first installed at the location indicated by pile 3 in Fig. 1. After lateral-load tests were completed on pile 3, the pile was pulled, the 15-ft long uninstrumented section was cut from the instrumented section, and the pile was installed again by procedures similar to those given above. In its second position, the 6-in. diameter pile is referred to as pile 4.

The 6-in. pile when tested as pile 4 was provided with a restrained-head during the load test as shown in Fig. 7. The rotational restraint was designed to provide a restraint at the loading flange which was about midway numerically between the completely fixed condition and the completely free condition. This degree of rotational restraint is believed representative for piles in jackets of offshore platforms.

Description of Tests

Both static and cyclic loads were applied to the test piles. The procedure for loading was similar to that used for the tests of laterally loaded piles in sand (1,2) and will not be discussed in detail here.

Summaries of the loading sequences on the piles are given in Tables 1, 2, 3 and 4 for test piles 1, 2, 3 and 4 respectively.

Method of Analysis

The analysis of laterally loaded piles, particularly in the design of offshore structures, is usually accomplished by the solution of Eq. 1.

$$EI \frac{d^4y}{dx^4} = p \qquad (1)$$

$$p = - E_s y$$

where

y = deflection

x = length along pile

EI = flexural stiffness of pile

p = soil resistance

E_s = soil modulus

Equation 1 can be solved readily (3,4,5,6,7) if the pile geometry and boundary conditions are known and if a family of curves can be developed showing p as a function of y.

The concept of p-y curves and the use of such curves has been discussed elsewhere in detail (2,5,7,8,9,10)) and will not be repeated here. Recommendations for developing p-y curves for a particular pile geometry and loading in soft and medium clay have been published (9,10) as have recommendations for piles in sand (2,8). With regard to laterally loaded piles in stiff clay, there is a publication dealing with the case where the water table is below the ground surface (11); however, this present paper is singular in that it presents recommendations for p-y curves for stiff clay that can be used in the analysis of piles supporting offshore structures.

Experimental p-y Curves

The procedures employed in developing criteria for p-y curves for stiff clay, using the results of these experiments, are as follows: obtain experimental p-y curves from field results, use theory as far as possible to describe soil behavior around a pile in stiff clay, and obtain empirical terms to produce agreement between the theory and experiments. The above steps will be described in this and the following sections.

With known boundary conditions at the top and the bottom of the pile, values of p and y can be computed at points along the pile from the experimental bending moment curves by solving the following equations:

$$y = \frac{M(x)}{EI} , \qquad (2)$$

$$p = \frac{d^2}{dx^2} M(x) . \qquad (3)$$

Equation 2 can be solved readily with good accuracy using numerical integration; however, special techniques must be employed in the solution of Eq. 3. The procedure employed by the writers was to assume that the soil modulus for a particular moment curve could be described by a two-parameter function (Eq. 4).

$$E_s = kx^n \qquad (4)$$

Non-dimensional solutions were obtained using Eq 4 (6) and numerical values of k and n were obtained by a fitting technique described elsewhere in detail.. (12) With values of k and n, Eq 1 can be solved to obtain values of p to go along with the values of y obtained from the solution of Eq 2. The procedure is repeated for each load and corresponding moment curve; thus, yielding families of p-y curves. There is, of course, some redundancy in the technique; e.g., values of y can be obtained from solutions of both Eqs 1 and 2; and the redundancy is employed to give the best possible curve fitting.

The families of p-y curves obtained by applying the techniques described above are shown in Figs. 8 through 11. The curves for short-term static loading of the first 24-in. diameter pile (Pile 1) is shown in Fig. 8. Curves for the cyclic load test of the second 24-in. diameter pile (Pile 2), reflecting the behavior of the soil for the maximum number of cycles for each load increment, are shown in Fig. 9. Figures 10 and 11 show the p-y curves for the 6-in. diameter pile (Piles 3 and 4), as obtained from the first installation and as obtained after pulling and redriving. The pile head was restrained against rotation for the results shown in Fig. 11.

While there is some irregularity in the shape of curves, the results appear to be quite good in view of the difficulty of the experimental and analytical problem. As a test of the accuracy of the p-y curves, the curves were used as input for a computer program that yields the pile behavior under each load increment. There was excellent agreement between the experimental results and the computed results. An example of the comparison is shown in Fig. 12. As may be seen, the experimental and computed results agree quite well for the full range of load increments and depths.

In all of the experimental p-y curves, the initial slope and the ultimate resistance increase with depth. A comparison of the p-y curves for the short-term static loading, Fig. 8, with the p-y curves for the cyclic loading, Fig. 9, shows that the soil resistances decrease as a result of cyclic loading. For the 6-in. diameter pile, a comparison of the p-y curves for the free-head loading, Fig. 10, with the p-y curves for the restrained-head loading, Fig. 11, shows a lower resistance at small depths but a larger resistance at large depths for the restrained-head case.

The general shape of a p-y curve in Fig. 8 agrees with what was expected. For any particular depth the initial part of the curve is relatively steep. At a particular deflection the ultimate soil resistance is developed, and beyond this point there is a reduction in soil resistance with continued deflection. With regard to the family of curves in Fig. 8, the slope of the initial part of the curve increases with depth as does the magnitude of the ultimate resistance.

An aspect of the family of curves in Fig. 8 which is surprising is the small deflection at which the ultimate soil resistance is attained. At a depth of 48 in. (two pile diameters), this deflection is approximately 0.2 in. which is less than one percent of the pile diameter. One gets the impression of a rather brittle behavior of the stiff clay.

Examination of the family of p-y curves in Fig. 9, obtained from the cyclic loading tests of a 24-in. diameter pile, shows that the shape of the initial part of a curve is similar to that of the corresponding curve obtained for static loading. The values of ultimate resistance for the cyclic curves are significantly less than the values for the static counterparts; also, for the cyclic curves the ultimate resistance was obtained with less deflection than for the static curves.

Of considerable surprise in Fig. 9 is the rather severe deterioration of the cyclic p-y curves beyond the point of ultimate resistance.

At a deflection of about 0.7 in. the soil resistance to a depth of 48 in. is reduced to virtually zero. At greater depths there is a sharp reduction in the soil resistance beyond a deflection of about 0.2 inch.

The sharp reduction in soil resistance for cyclic loading beyond the point of ultimate resistance is a cause of some concern regarding the design of laterally loaded piles in stiff clays to sustain storm loadings. While the deterioration of soil resistance as a result of cyclic loadings is certainly severe in this case, there are three points to be made which give a somewhat more optimistic view of these cyclic p-y curves.

1. The curves represent a lower limiting value of soil resistance, since a very severe cyclic loading condition was employed. In the testing procedure, a particular load increment was repeated until the pile had stabilized at a particular maximum deflection or until 100 cycles of loading had been applied. It would be a severe storm where the design wave could act against a structure as many as 100 times.
2. Regardless of the degree of deterioration of the p-y curves to a given depth, the soil below that depth still has the capability of resisting the pile deflection. At the maximum load applied in the cyclic test of pile 2, the resistance of the soil in the top 48 in. had apparently been destroyed, but the soil at a depth of 84 in. was exhibiting a resistance of about 600 lb/in. and the soil at a depth of 108 in. was showing a resistance of about 2000 lb/inch.
3. If, after cyclic loading under the maximum load had been completed, it had been possible to impose additional static deflection on the pile, the soil resistance even at the shallow depths would have risen perhaps to a value equal to the ultimate previously attained, depending on the amount of the additional deflection. This phenomenon is due to the fact that the cyclic loading pushed back and eroded the soil and opened up a space between the pile and the soil. Deflecting the pile through this space and firmly against the intact soil would again develop soil resistance at the shallow depths. Thus, the pile might be able to sustain a small number of cycles of loading from a significantly larger wave than the nominal design wave.

The p-y curves in Fig. 10 and 11 for static loading of the 6-in. diameter pile are similar in shape to the static p-y curves for the 24-in. diameter pile (Fig. 8). Some results of a comparative study of the static p-y curves for the 6-in. diameter pile and the 24-in. diameter pile will be given in the section on development of soil criteria.

The families of p-y curves in Figs. 10 and 11 were developed from data obtained from static loading of the 6-in. diameter pile. Pile 3 (curves in Fig. 10) was a free-head pile while pile 4 (curves in Fig. 11) was a restrained-head pile. For pile 4 the pile head was restrained against rotation by a frame which was adjusted to produce a top fixity such that the ratio of bending moment to pile slope M/S was equal to 3.5 EI/L.

Comparison of the curves shown in Figs. 10 and 11 shows that soil resistance for depths of 12 in. and 24 in. are less for the restrained-head case than for the free-head case. The p-y curve for a depth of 36 in. is about the same for both tests, while the curves for depths of 48 in. and 60 in. are somewhat stronger for the restrained-head case than for the free-head case.

No conclusive explanation can presently be advanced to account for the differences in the p-y curves. While these differences may be due to the difference in pile head conditions, it is possible that variation in soil properties between the two locations could account for part of the differences noted in the curves. There is a further possibility of differences in the disturbance of the soil at the two locations because of the pile driving.

From the standpoint of pile design, the difference in the p-y curves from pile 3 and pile 4 is small, and it was decided that the amount of data is insufficient to recommend any differences in criteria for p-y curves for free-head and for restrained-head piles.

Development of Procedure for Predicting Soil Behavior

The experimental p-y curves presented in Figs. 8 through 11 can be used to predict the behavior of laterally loaded piles in soils having physical properties like those at the test site, but methods are needed, of course, for use at any site where there is stiff clay. There are uncertainties in extrapolating the results from one site into a general set of recommendations but theories of soil behavior will be used to reduce those uncertainties as much as possible.

Some preliminary studies of the experimental p-y curves were undertaken with the view that a diameter effect could be established using results from the tests of the 6-in. and 24-in. diameter piles. However, these studies were unproductive and it was decided to base the recommendations for soil behavior principally on results of the 24-in. diameter tests. Reference will be made later to the 6-in. diameter test results.

In the development of recommendations for soil behavior, characteristic shapes of the p-y curves for both static and cyclic loading are selected, as shown in Fig. 13. The static curve (Fig. 13a) consists of an initial straight portion, shown as the section from the origin to point 1; two parabolic sections, from point 1 to point 2 and from point 2 to point 3; and two straight portions, from point 3 to point 4 and a horizontal line beyond point 4. The ultimate static soil resistance occurs in the parabolic section of the curve between point 2 and point 3.

The characteristic shape of the cyclic curve, as shown in Fig. 13b, consists of an initial straight portion, shown as the section from the origin to point 1; a parabolic section, from point 1 to point 2; and two straight portions, from point 2 to point 3 and a horizontal line beyond point 3. The ultimate cyclic soil resistance occurs in the parabolic section of the curve.

A straight-line relationship between low magnitudes of soil stress and strain is frequently observed; therefore, an initial straight portion of a p-y curve as revealed by Figs. 8 through 11 is to be expected. The slopes of these initial straight lines were determined from the equation:

$$E_{si} = \frac{p_i}{y_i} \quad (5)$$

where

E_{si} = initial soil modulus, lb/sq in.

p_i and y_i = coordinates of point on initial portion of p-y curve, lb/in. and in., respectively.

Values of E_{si} corresponding to values of p_i and y_i at different depths x have been plotted in Fig. 14 from static and from cyclic p-y curves. As shown in Fig. 14, E_{si} can be expressed as a function of the depth x, such that

$$E_{si} = kx \quad (6)$$

Equation 6 was used to obtain values of k for both static and cyclic cases, with the following results:

k_s (static) = 1000 lb/cu in

k_c (cyclic) = 400 lb/cu in.

Values of k should vary with the undrained shear strength for both static and cyclic cases; recommended values of k are shown in Table 5. The numerical values in the center column of Table 5 are derived from results of this research program. The other values are suggested after study of work by Terzaghi (13).

A study of Figs. 8 and 9 shows that for a number of the experimental p-y curves, there is a well defined value of ultimate soil resistances that increases with depth. The idea of a wedge of clay moving up and out from a pile has been used previously to obtain an approximate theoretical value of the ultimate soil resistance near the ground surface (14), and the following expression was obtained.*

$$p_{c1} = 2\, c_a\, b + \gamma'\, b\, H + 2.83\, c_a\, H \quad (7)$$

where

p_{c1} = ultimate soil resistance at depth H
c_a = average undrained shear strength of clay over depth H
b = diameter (or width) of pile (25.25 in. for 24-in. diameter piles)
γ' = submerged unit weight of soil (assuming water surface to be above ground surface)

The assumptions made in the derivation of Eq 7 are: the clay has a constant shear strength over the depth H, the wedge of soil moving up and out can be defined by three plane surfaces and a surface next to the pile, the undrained shear strength of the clay is fully developed along the sliding surfaces, the bottom surface of the wedge is at an angle of 45° with the horizontal, and there is no vertical force between the pile and the upward-moving soil. The simplified failure model and the number of assumptions involved in the derivation of Eq 7 leads to considerable uncertainty about the validity of the expression; however, the expression is based on a rational model for soil behavior and thus should involve the important variables.

At some point below the ground surface the soil fails by flowing horizontally around the pile. Again, a simplified but rational model is employed. Blocks of soil around the pile and the stresses against the pile are computed on the assumptions that each of the blocks of soil has failed (14). The resulting expression is shown in Eq 8.

$$p_{c2} = 11\, c\, b \quad (8)$$

where

c = the undrained shear strength of the clay at the depth for the p-y curve.

Ultimate soil resistance values were computed by using Eqs 8 and 9 and it was found that the values were considerably larger than the values from experiment (see Figs. 8 and 9). It was, therefore, decided to adjust the ultimate resistance values empirically by dividing the observed ultimate soil resistance by the computed ultimate soil resistance as follows:

$$A = \frac{(p_u)_s}{p_c} \quad (9)$$

$$B = \frac{(p_u)_c}{p_c} \quad (10)$$

*Matlock (9) obtained a similar expression for the ultimate soil resistance near the ground surface for soft clay.

where

A = empirical adjustment factor for static loading

B = empirical adjustment factor for cyclic loading

p_c = ultimate resistance from theory

$(p_u)_s$ = ultimate resistance measured for static loading

$(p_u)_c$ = ultimate resistance measured for cyclic loading.

The experimentally determined values of the coefficients A and B are shown in Fig. 15. Fig. 16 shows observed and computed values of ultimate soil resistance versus depth. As expected, the agreement between observed and computed values is excellent because of the use of the empirical A and B coefficients. No experimental values of ultimate were obtained where the soil failed by flowing horizontally around the pile.

With regard to the remainder of the definition of the p-y curves, a concept used previously is employed (9,10,15); that a load deflection curve can be related to the stress-strain curve for a laboratory specimen. A significant parameter defining the laboratory stress-strain curve is the strain, ε, corresponding to a stress of 50 percent of the ultimate stress. In the absence of laboratory stress-strain curves for the soil, the representative values of ε_c given in Table 6 may be used. A parameter y_c is defined as follows for use in the design recommendations,

$$y_c = \varepsilon_c \, b \tag{11}$$

The equation of a parabola going through the origin on the static p-y curve shown in Fig. 11 is

$$p = 0.5 \, p_c \left(\frac{y}{y_c}\right)^{0.5} \tag{12}$$

The parabolic shape of the static p-y curve in Fig. 17 is assumed to begin at the intersection of the straight line, defined with the slope of E_{si}, and the parabola, defined by Eq 12. This parabola continues to a point defined by a deflection equal to $A\, y_c$, where A is given in Fig. 15 for the non-dimensional depth x/b for which the p-y curve is desired.

At the deflection corresponding to $A\, y_c$ the parabola defined by Eq 12 is modified by an offset which has the value

$$p_{offset} = 0.055 \, p_c \left(\frac{y - A\, y_c}{A\, y_c}\right)^{1.25} \tag{13}$$

This offset to the p-y curve defined by Eq 12 continues to the deflection corresponding to $6\, A\, y_c$. At this deflection the p-y curve assumes a straight line with a slope equal to

$$E_{ss} = - \frac{0.0625 \, p_c}{y_c} \tag{14}$$

This straight line continues to a deflection equal to $18\, A\, y_c$ at which point the curve becomes a horizontal line.

A p-y curve representative of experimental p-y curves for cyclic loadings is shown in Fig. 18. A deflection y_p is defined such that

$$y_p = 4.1\, A\, y_c \tag{15}$$

The parabola in the p-y curve is expressed by

$$p = B\, p_c \left[1 - \left|\frac{y - 0.5\, y_p}{0.45\, y_p}\right|^{2.5}\right] \tag{16}$$

This parabola begins in the p-y curve at the intersection of Eq 16 with the line defined by the slope E_{si} passing through the origin. The parabola continues to a value of deflection equal to $0.6\, y_p$. At this point the p-y curve is represented by a straight line with a slope equal to

$$E_{sc} = - \frac{0.085\, p_c}{y_c} \tag{17}$$

The straight line with the slope defined by Eq 17 continues to the deflection equal to $1.8\, y_p$ at which point the p-y curve becomes horizontal.

This completes the recommendations for the development of p-y curves for stiff clay for static and for cyclic loading. A step-by-step procedure is presented in the next section for convenience.

Step-by-Step Procedure for Developing p-y Curves

The procedure given below is confined to the development of one p-y curve at depth H. A family of p-y curves will be needed in the analysis of a laterally loaded pile.

Procedure for Developing p-y Curves for Static Loading

1. Obtain values for undrained soil shear strengths c, soil submerged unit weight γ, and pile diameter b from ground surface to depth H.
2. Compute the average undrained soil shear strength c_a over the depth H.
3. Use the following equations for computing soil resistance at depth H:

   a. Ultimate soil resistance near ground surface,

   $$p_{c1} = 2\, c_a\, b + \gamma'\, b\, H + 2.83\, c_a\, H \tag{7}$$

   b. Ultimate soil resistance well below the ground surface,

   $$p_{c2} = 11\, c\, b \tag{8}$$

   Use the smaller of Eq (7) or (8) for the value of p_c.
4. Choose the appropriate value of A from Fig. 15 for the particular non-dimen-

sional depth.

5. Establish the initial straight line portion of the p-y curve,

$$p = k \; x \; y \tag{18}$$

Use the appropriate value of k from Table 5.

6. Compute the following:

$$y_c = \varepsilon_c \; b \tag{11}$$

Use an appropriate value of ε_c from Table 6.

7. Establish the first parabolic portion of the p-y curve,

$$p = 0.5 \; p_c \; (\frac{y}{y_c})^{0.5} \tag{12}$$

Intersection with Eq 18 $\leq y \leq A \; y_c$ (if there is no intersection, Eq 12 controls).

8. Establish the second parabolic portion of the p-y curve,

$$p = 0.5 \; p_c \; (\frac{y}{y_c})^{0.5}$$

$$- 0.055 \; p_c \; (\frac{y - A \; y_c}{A \; y_c})^{1.25},$$

$$A \; y_c \leq y \leq 6 \; A \; y_c \tag{19}$$

9. Establish the next straight-line portion of the p-y curve,

$$p = 0.5 \; p_c \; (6A)^{0.5} - 0.411 \; p_c$$

$$- \frac{0.0625}{y_c} \; p_c \; (y - 6 \; A \; y_c),$$

$$6 \; A \; y_c \leq y \leq 18 \; A \; y_c \tag{20}$$

10. Establish the final straight-line portion of the p-y curve,

$$p = 0.5 \; p_c \; (6A)^{0.5} - 0.411 \; p_c - 0.75 \; p_c \; A,$$

$$18 \; A \; y_c \leq y \tag{21}$$

Procedure for Developing p-y Curves for Cyclic Loading

1. Steps 1, 2, 3, and 5 are the same as for the static case.
4. Choose the appropriate value of B from Fig. 15 for the particular non-dimensional depth.
6. Compute the following:

$$y_c = \varepsilon_c \; b \tag{11}$$

$$y_p = 4.1 \; A \; y_c \tag{15}$$

Use an appropriate value of ε_c from Table 2.

7. Establish the parabolic portion of the p-y curve,

$$p = B \; p_c \left[1 - \left| \frac{y - 0.45 \; y_p}{0.45 \; y_p} \right|^{2.5} \right] \tag{16}$$

Intersection with Eq 18 $\leq y \leq 0.6 \; y_p$ (if there is no intersection, Eq 16 controls).

8. Establish the next straight-line portion of the p-y curve,

$$p = 0.936 \; B \; p_c - \frac{0.085}{y_c} \; p_c \; (y - 0.6 \; y_p),$$

$$0.6 \; y_p \leq y \leq 1.8 \; y_p \tag{22}$$

9. Establish the final straight-line portion of the p-y curve,

$$p = 0.936 \; B \; p_c - \frac{0.102}{y_c} \; p_c \; y_p,$$

$$1.8 \; y_p \leq y \tag{23}$$

Comparison of Results of Proposed Method with Experimental Results

Measured and computed values of maximum bending moment as a function of lateral load for static loading are shown in Fig. 19. Curves in Fig. 20 show the comparison between measured and computed values of deflection at the goundline. Figure 21 shows measured and computed bending moment curves as a function of depth for static loading and for the maximum lateral load on the pile. A study of curves in Figs. 19 through 21 shows that the recommended method for computing p-y curves for static loading produces excellent agreement between measured and computed results for the tests of 24-in. diameter piles.

Figures 22 and 23 show comparisons between measured and computed results for the 6-in.diameter pile that was tested at the site. While there is reasonable agreement for the maximum bending moment, the agreement for deflection at groundline is poor. No good reason was developed for the poor results shown in Fig. 23; however, in view of the good comparisons demonstrated for other results, the comparison shown in Fig. 23 is not considered to be of great importance.

Comparisons between measured and computed results for cyclic loading of the 24-in. diameter pile are shown in Figs. 24 through 26. As for the static loading, agreement between measured and computed results is excellent.

On the basis of the comparisons discussed above, the procedure that was developed for predicting p-y curves is valid for the test site.

Concluding Comments

The methods that are described for predicting p-y curves for stiff clay, for static and for cyclic loading, involve the readily identifiable parameters that relate to the behavior of the soil around a laterally loaded pile. The development of methods for predicting p-y curves for all manner of stiff clays is a complex problem and will probably require the performance of a number of full-scale tests as described herein. Therefore, care should be employed in the use of the methods presented for predicting p-y curves for stiff clay.

Acknowledgement

Appreciation is extended to Shell Development Company for granting permission to release information on these studies.

References

1. Cox, William R., Lymon C. Reese, and Berry R. Grubbs, "Field Testing of Laterally Loaded Piles in Sand," Paper No. OTC 2079, Proceedings, Sixth Annual Offshore Technology Conference, Houston, Texas, 1974, Vol. 2, pp. 459-472.

2. Reese, Lymon C., William R. Cox, and Francis D. Koop, "Analysis of Laterally Loaded Piles in Sand," Paper No. OTC 2080, Proceedings, Sixth Annual Offshore Technology Conference, Houston, Texas, 1974, Vol. 2, pp. 473-83.

3. Hetenyi, M., Beams on Elastic Foundation, University of Michigan Press, Ann Arbor, Michigan, 1946.

4. Gleser, Sol M., "Lateral Load Tests on Vertical Fixed-head and Free-head Piles," Special Technical Publication 154, American Society for Testing Materials, 1953, p. 75.

5. Reese, Lymon C., and Hudson Matlock, "Non-Dimensional Solutions for Laterally Loaded Piles with Soil Modulus Assumed Proportional to Depth," Proceedings, Eighth Texas Conference on Soil Mechanics and Foundation Engineering, Austin, Texas, 1956.

6. Matlock, Hudson, and Lymon C. Reese, "Generalized Solutions for Laterally Loaded Piles," Journal of the Soil Mechanics and Foundations Division, American Society of Civil Engineers, October, 1960, p. 63.

7. Matlock, Hudson, and Lymon C. Reese, "Foundation Analysis of Offshore Pile-Supported Structures," Proceedings, Fifth International Conference, International Society of Soil Mechanics and Foundation Engineering, Paris, Vol 2, 1961, p. 91.

8. Parker, Frazier, and Lymon C. Reese, "Lateral Pile-Soil Interaction Curves for Sand," Proceedings, The International Symposium on the Engineering Properties of Sea-Floor Soils and Their Geophysical Identification, University of Washington, Seattle, Washington, July 25, 1971.

9. Matlock Hudson, "Correlations for Design of Laterally Loaded Piles in Soft Clay," Paper No. OTC 1204, Proceedings, Second Annual Offshore Technology Conference, Houston, Texas, 1970, Vol. 1, pp. 577-594.

10. McClelland, Bramlette, and J. A. Focht, Jr., "Soil Modulus for Laterally Loaded Piles," Transactions, American Society of Civil Engineers, Vol. 123, 1958, pp. 1049-1063.

11. Reese, Lymon C., and Robert C. Welch, "Lateral Loading of Deep Foundations in Stiff Clay," submitted to the Publications Committee, Geotechnical Engineering Division, American Society of Civil Engineers, November, 1974.

12. Reese, Lymon C., and William R. Cox, "Soil Behavior from Analysis of Tests of Uninstrumented Piles Under Lateral Loading," Performance of Deep Foundations, ASTM STP 444, American Society of Civil Engineers, Vol. 123, pp. 161-176.

13. Terzaghi, Karl, "Evaluation of Coefficients of Subgrade Reaction," Geotechnique, Vol. 5, No. 4, December, 1955, pp. 297-326.

14. Reese, Lymon C., Discussion of "Soil Modulus for Laterally Loaded Piles," by Bramlette McClelland and John A. Focht, Jr., Transactions, American Society of Civil Engineers, Vol. 123, 1958, pp. 1071-1074.

15. Skempton, "The Bearing Capacity of Clays," Proceedings, Building Research Congress, England, 1951.

TABLE 1 - SUMMARY OF STATIC AND CYCLIC TEST LOADS FOR PILE 1

Type of Load	Loads and Cycle Numbers Corresponding to Data Recording			
	Load, Kips	Number of Cycles Major Direction	Number of Cycles Minor Direction	Ratio of Major To Minor Load
Static . . . . . . (June 12, 1967)	0,2.6,4.8,6.8, 9.2,11.2,13.1, 14.9,17.4,20.6, 25.1,29.7,35.2, 40.4,45,50.1, 59.8, 61,71.1, 79.9,90,100,108, 119,128,134,101, 73,51.5,26,6.3, 0			
Cyclic	0	0	**0,6	*3
	2	0,6		
	3.3	0,5,10		
	10	0,6,10		
	15	0,13		
	19.6	0,20		
	30.1	0,10		
	38.5	0,11		
	50.5	0,10		
	59.8	0,10		
	71	0,10		
	80.2	0,10,15,20		
	101	0,10,15,20,25		
	116.5	0,10,20,25,30		
	113	25,30		
	120.4	0,10,20,31,40, 50,60,70		
	0	0		
Cyclic . . . . . . (June 16, 1967)	0	0		3
	20	10		
	40	10		
	60	10		
	80	10		
	96	10		
	110	10		
	120	10		
	126	10		
	134.5	10		
	0	0		
	118	20		
	116	20	20	
	114.6	20		
	0	0		
Cyclic . . . . . . (June 21, 1967)	0	0		3
	100	0,100,200, 300,400, 500	0,500	
	0	0		

*Ratio was constant throughout the load series.

**Data were recorded at noted cycle only although a minor load was applied at each cycle.

TABLE 2 - SUMMARY OF CYCLIC AND STATIC TEST LOADS FOR PILE 2

Type of Load	Loads and Cycle Numbers Corresponding to Data Recording			
	Load, Kips	Number of Cycles Major Direction	Number of Cycles Minor Direction	Ratio of Major to Minor Load
Cyclic . . . . (July 12, 1967)	0	0		3
	5	1,6,10,21		
	10	1,5,10,20		
	15	1,10,20		
	20	1,10,20,30		
	27.5	1,10,20,30		
	35	1,12,20,30		
	42.5	1,10,20,30		
	50	1,10,20,30,40		
	57.5	1,20,40,50,60,		
	65	1,20,40,60		
	72.5	1,20,40,60,80 100		
	80	1,20,40,60,80, 100		
	87.5	1,20,40,60,80, 100		
	95	1,20,40,60,80 100	100	
	97.5	1,20,40,60,80 100	100	
	0	0		
Static . . . (July 13, 1967)	0,5,10,15, 20,27.5,35, 42.5,50,57.5, 65,72.5,80, 87.5,95,97.5, 100,102.5, 105,107.5,0			

TABLE 3 - SUMMARY OF STATIC AND CYCLIC TEST LOADS FOR PILE 3

Type of Load	Loads and Cycle Numbers Corresponding to Data Recording			
	Load, Kips	Number of Cycles Major Direction	Number of Cycles Minor Direction	Ratio of Major to Minor Load
Static . . . . . (June 27, 1967)	.8,2,2.75, 4,5,6,7, 8,9,9.5, 10,10.5,8, 5,2,0			
Cyclic . . . . . (June 28, 1967)	0	0		3
	.5	1,10,20		
	1	1,11,20		
	1.75	1,10,20		
	2.5	1,10,20		
	3.25	1,12,20		
	4	1,10,20,30,40		
	4.75	1,20,30,40		
	5.5	1,20,40,50		
	6.25	1,20,40,60,70 80,90,100		
	7	1,20,40,60,80 100		
	7.5	1,20,40,60,100	100	
	0	0		

TABLE 4 - SUMMARY OF STATIC AND CYCLIC TEST LOADS FOR PILE 4

Type of Load	Loads and Cycle Numbers Corresponding to Data Recording			
	Load, Kips	Number of Cycles: Major Direction	Number of Cycles: Minor Direction	Ratio of Major to Minor Load
Static . . . . . (Sept 1,1967)	0,1,2,3,4, 5,6,7,8,9, 10,11,12,13, 14,15,16,17, 10,5,0			
Cyclic . . . . . (Sept 2,1967)	0	0		3
	1	0,25		
	2	0,10		
	3	0,10		
	4	0,10		
	5	0,10,20,30		
	6	0,10,20,30,40, 50,60		
	7	0,20,40,60,80		
	8	0,20,40,60,80		
	9	0,40,80,100		
	10	0,40,80,100		
	11	0,40,80,100		
	12	0,40,80,100		
	13	0,40,80,100		
	14	0,40,80,100		
	0			

TABLE 5-RECOMMENDED VALUES OF K FOR STIFF CLAYS

	Average Undrained Shear Strength* ton/ft^2		
	0.5-1	1-2	2.4
k_s (Static) lb/in^3	500	1000	2000
k_c (Cyclic) lb/in^3	200	400	800

*The average shear strength should be computed from the shear strength of the soil to a depth of 5 pile diameters.

TABLE 6 - REPRESENTATIVE VALUES OF ε_c FOR STIFF CLAYS

	Average Undrained Shear Strength ton/ft^2		
	0.5-1	1-2	2-4
ε_c (in./in.)	0.007	0.005	0.004

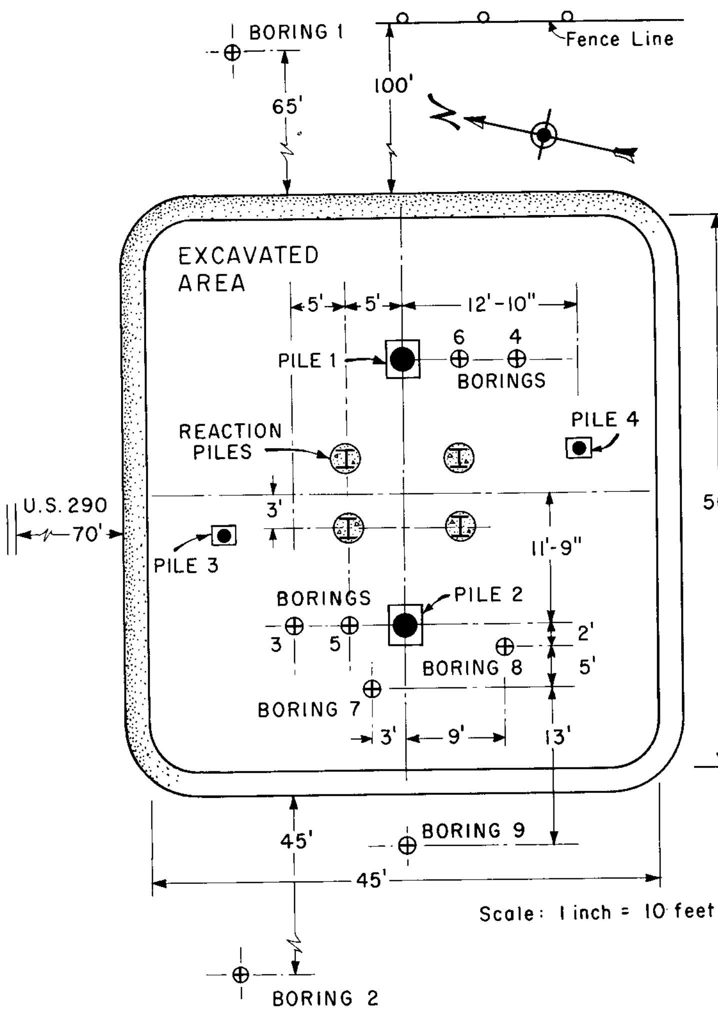

Fig. 1 - Drawing of test area showing locations of borings and piles.

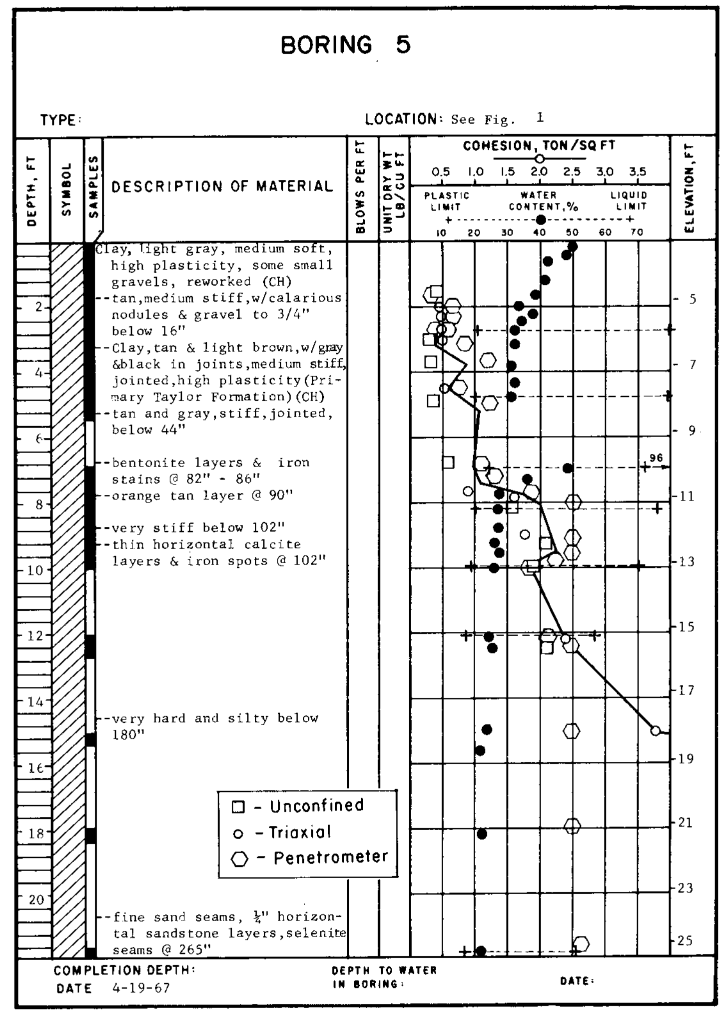

Fig. 2 - Log of boring 5.

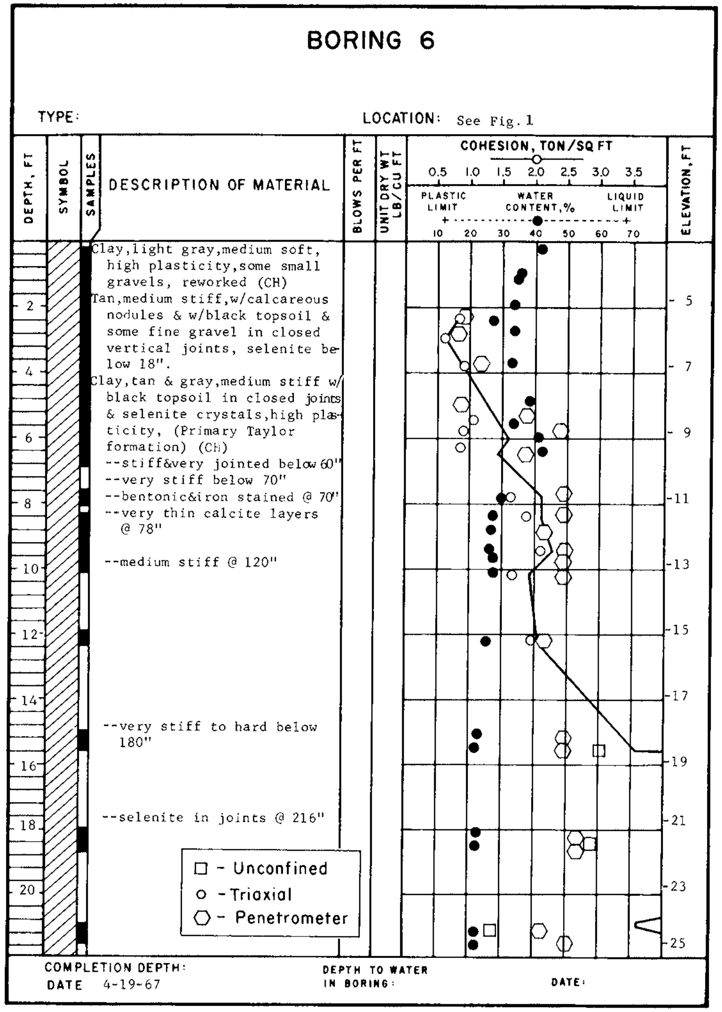

Fig. 3 - Log of boring 6.

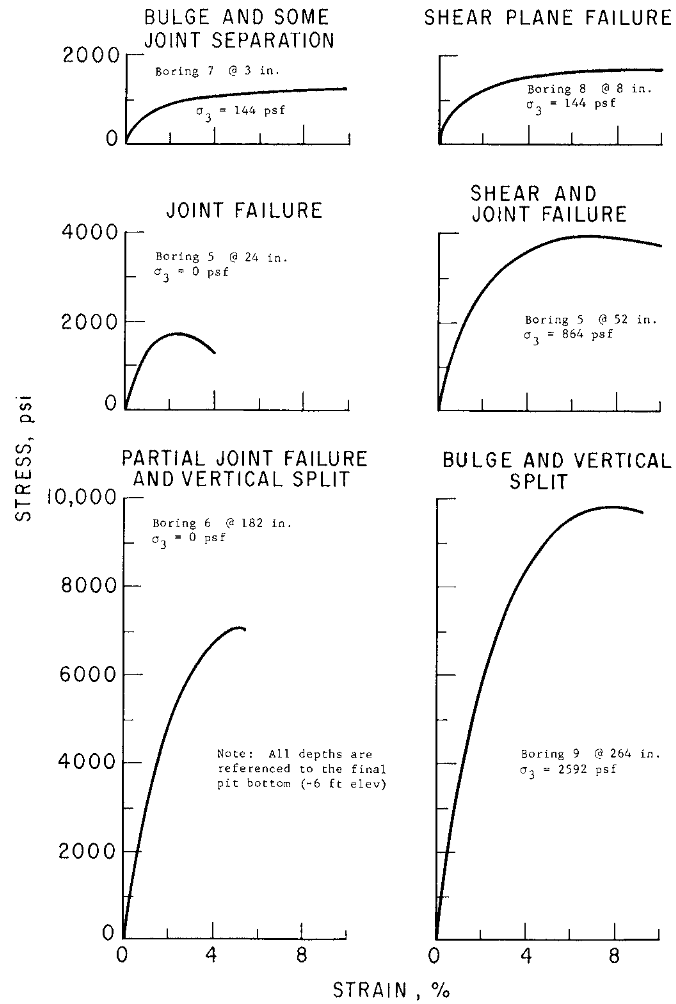

Fig. 4 - Typical stress-strain curves of soil samples.

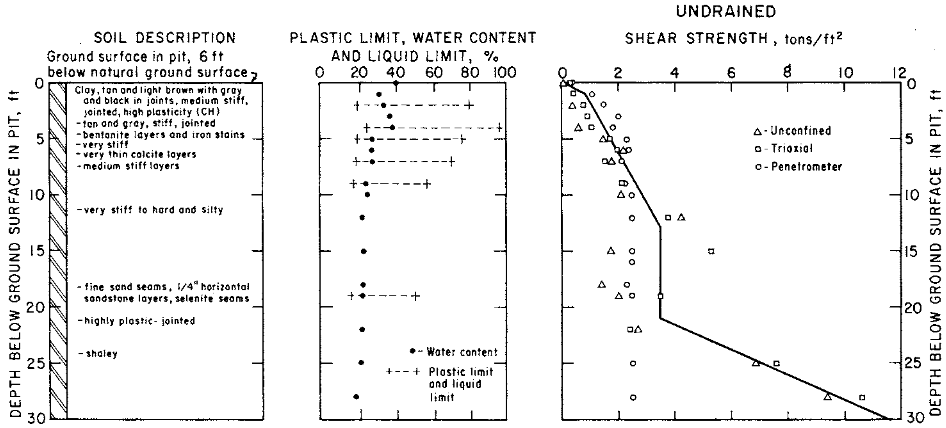

Fig. 5 - Composite soil profile.

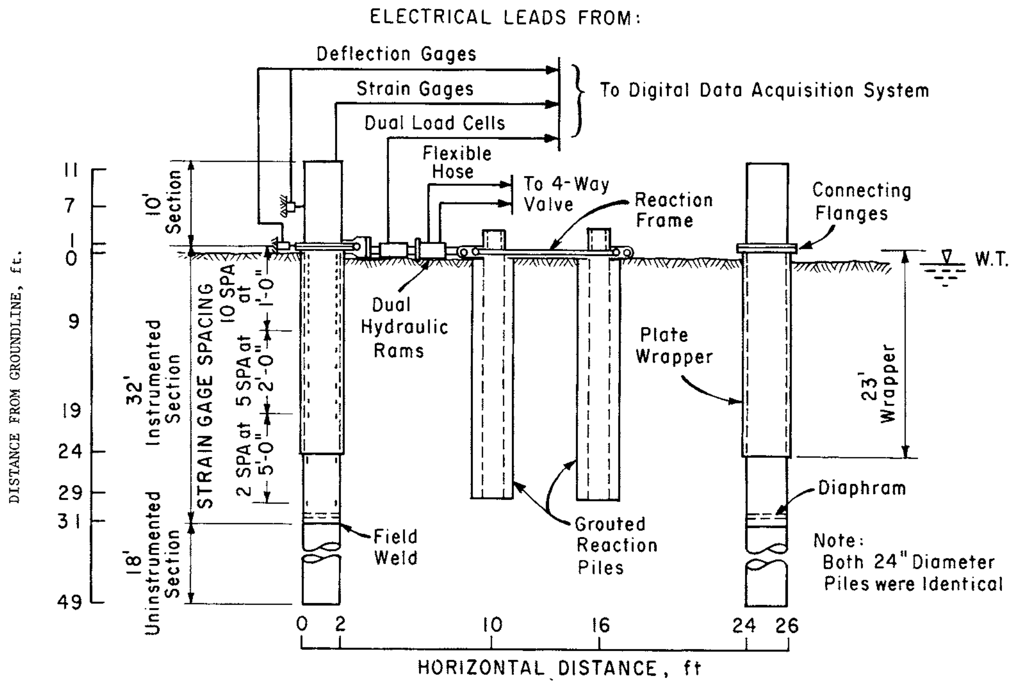

Fig. 6 - Test set-up for 24-in diameter test piles.

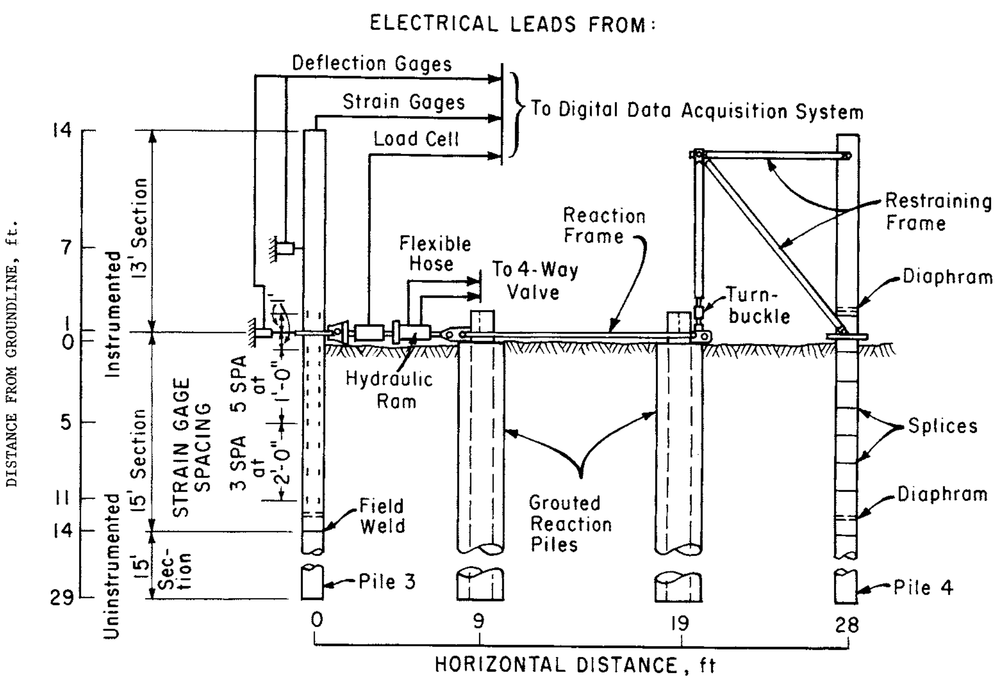

Fig. 7 - Test set-up for 6-in diameter test pile.

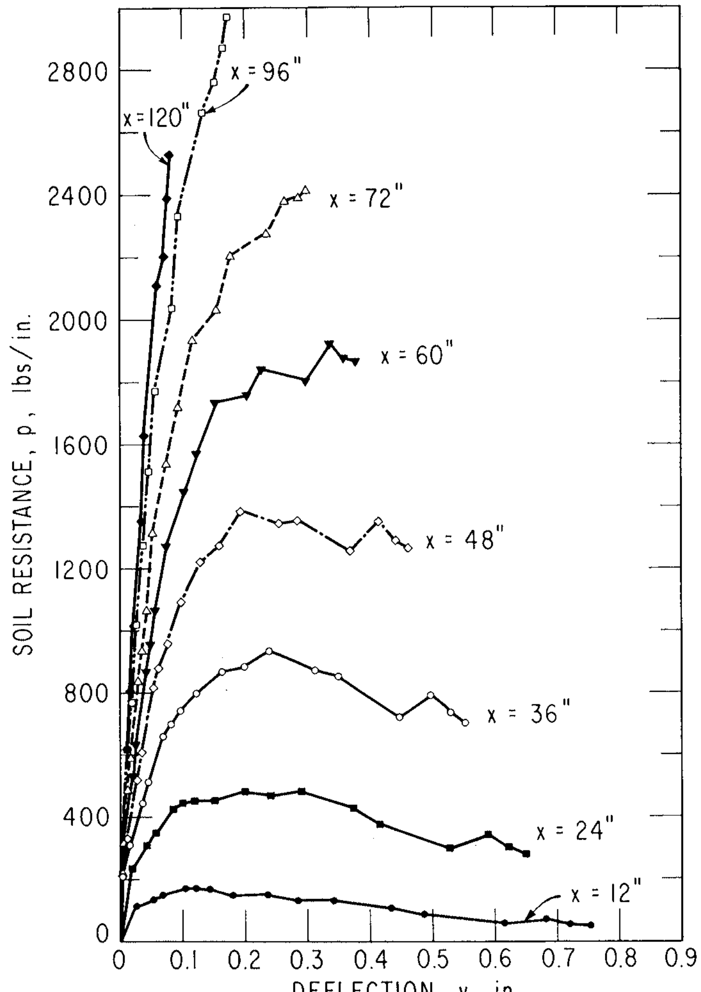

Fig. 8 - P-Y curves developed from static-load test on 24-in diameter pile. (Pile 1).

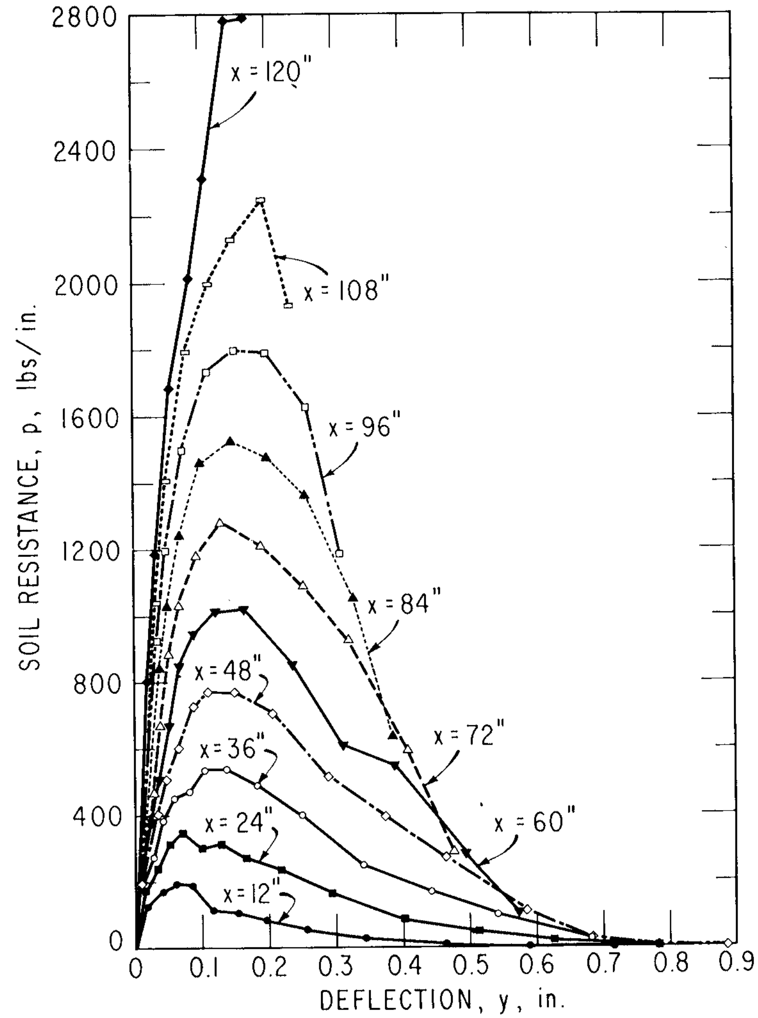

Fig. 9 - P-Y curves developed from cyclic-load test on 24-in diameter pile. (Pile 2).

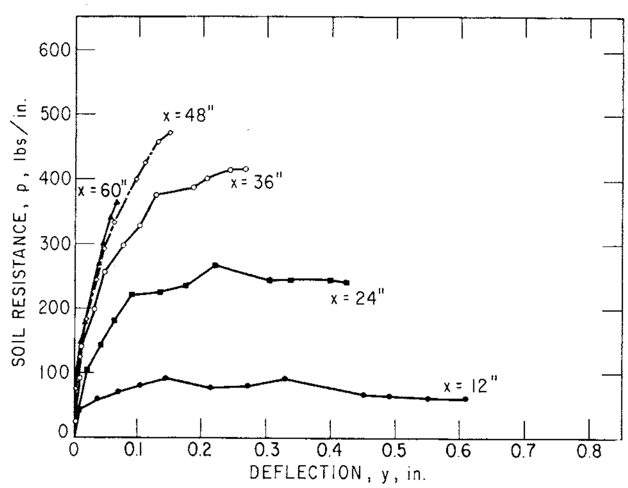

Fig. 10 - P-Y curves developed from static-load test on 6-in diameter pile (Pile 3).

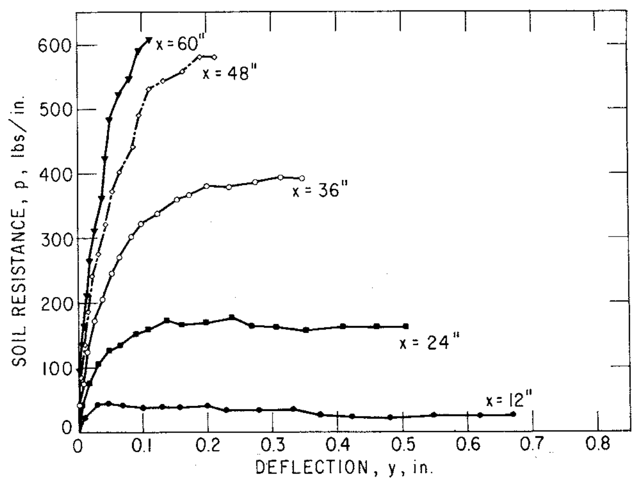

Fig. 11 - P-Y curves developed from static-load test on 6-in diameter pile (Pile 4).

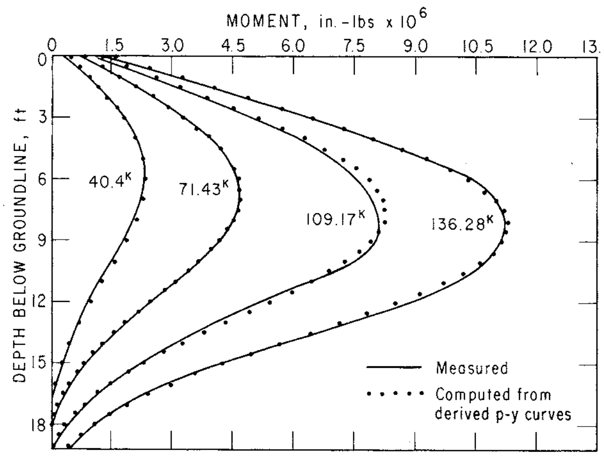

Fig. 12 - Comparison of computed moment curves with measured moment curves for static test on 24-in diameter pile (Pile 1).

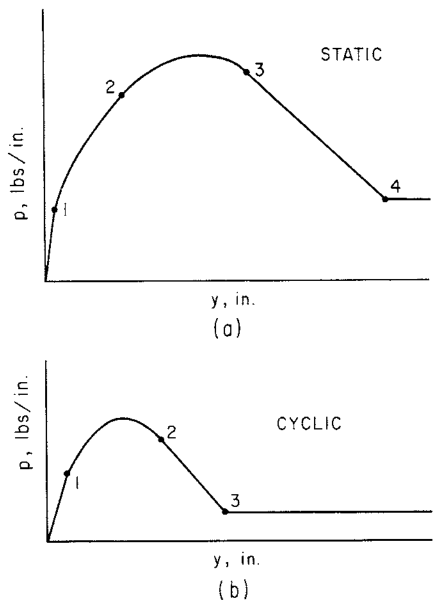

Fig. 13 - Characteristic shape of proposed p-y criteria for stiff clay. (a) Static and (b) Cyclic.

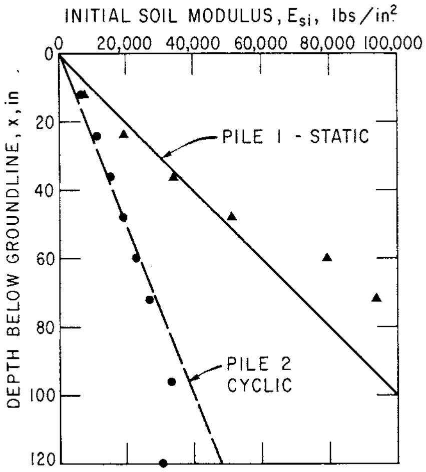

Fig. 14 - Initial soil modulus vs. depth.

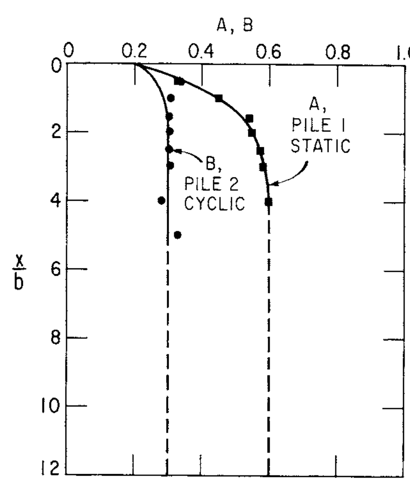

Fig. 15 - Non-dimensional coefficients A and B of ultimate soil resistance vs non-dimensional depth.

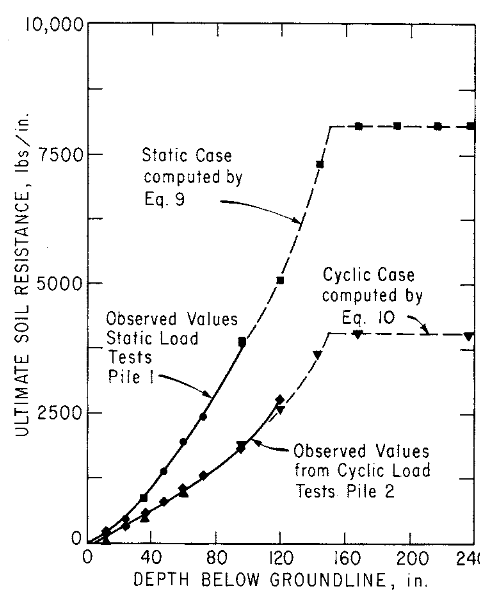

Fig. 16 - Observed and computed values of ultimate soil resistance vs depth.

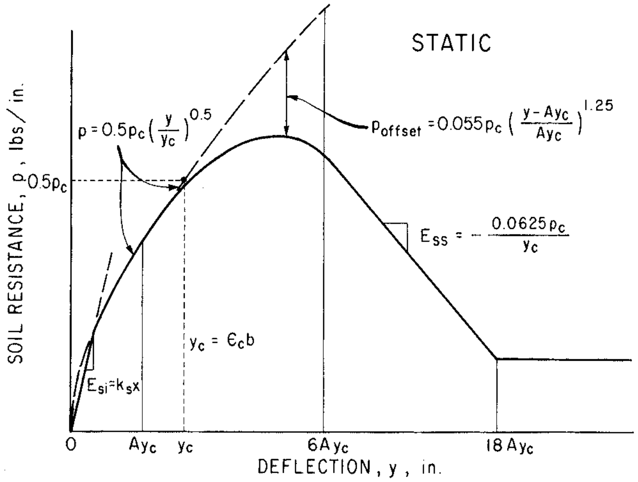

Fig. 17 - Characteristic shape of proposed p-y criteria for static loading in stiff clay.

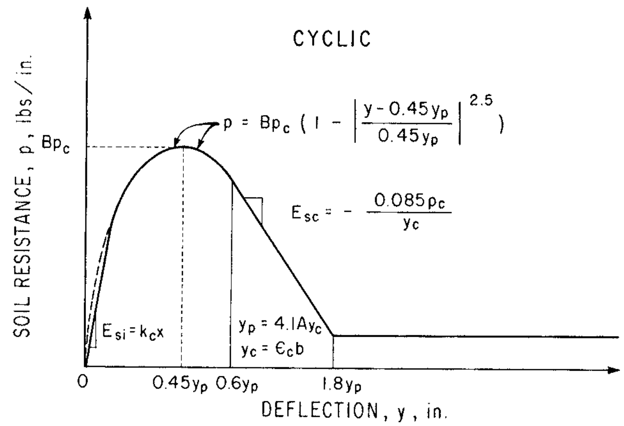

Fig. 18 - Characteristic shape of proposed p-y criteria for cyclic loading in stiff clay.

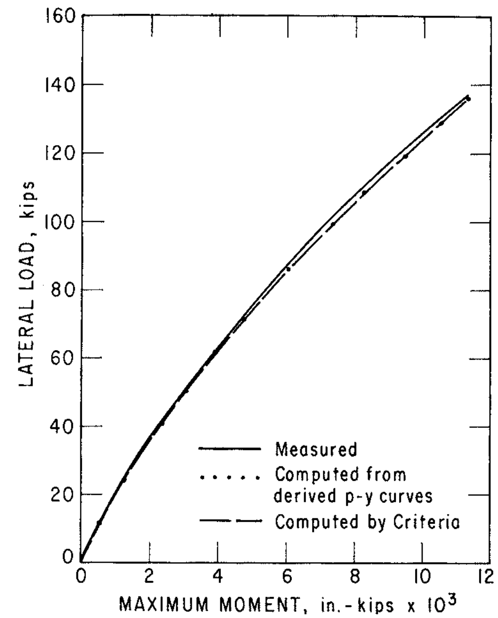

Fig. 19 - Comparison between measured an computed values of maximum bending moment f static loading, 24-in diameter pile. (Pile

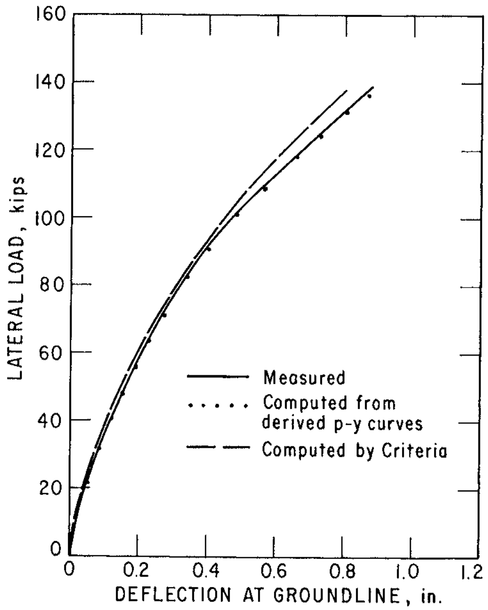

Fig. 20 - Comparison between measured and computed values of deflection at groundline for static loading, 24-in diameter pile. (Pile I).

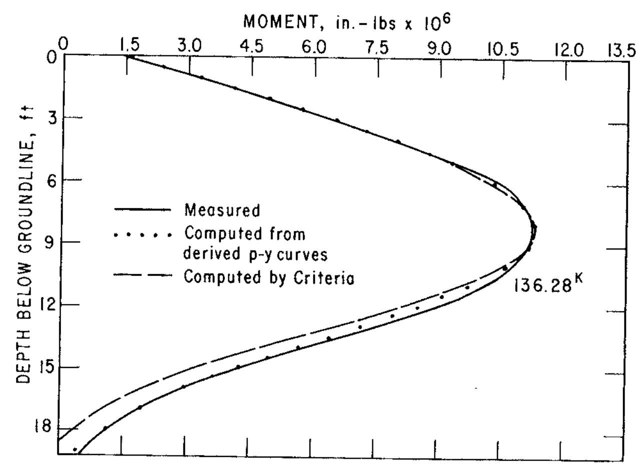

Fig. 21 - Comparison between measured and computed bending moment curves for static loading and for the maximum lateral load, 24-in diameter pile. (Pile I).

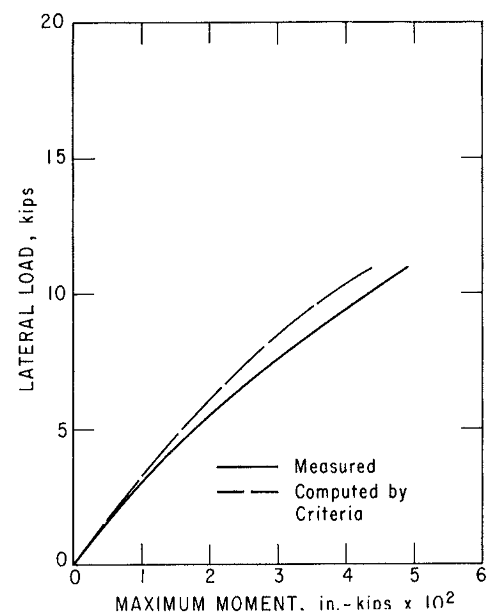

Fig. 22 - Comparison between measured and computed values of maximum bending moment for static loading, 6-in diameter pile. (Pile 3).

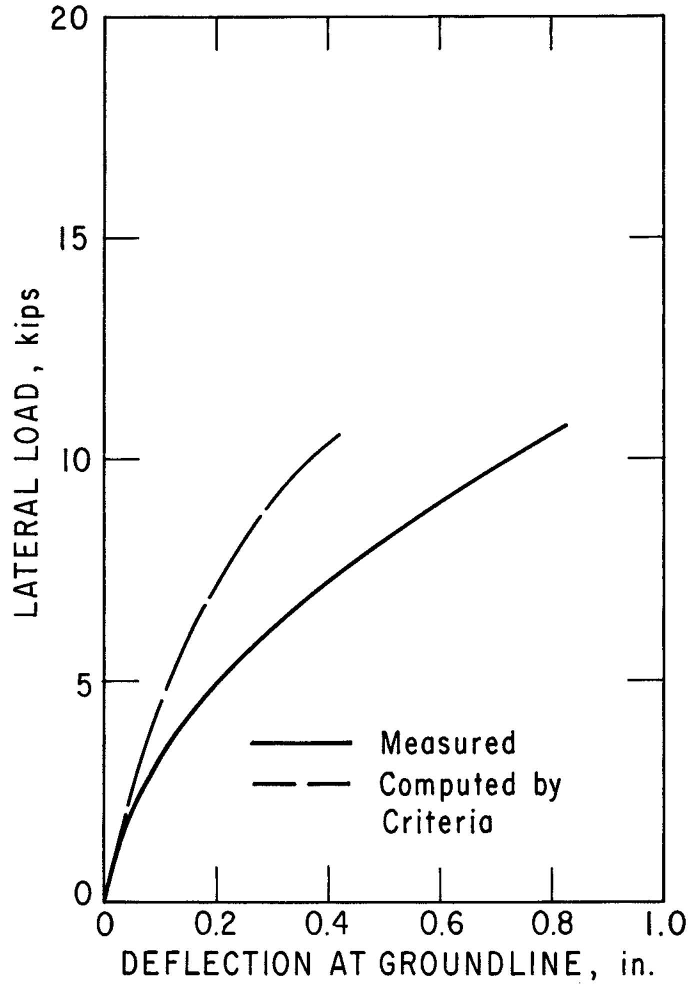

Fig. 23 - Comparison between measured and computed values of deflection at groundline for static loading, 6-in diameter pile. (Pile 3).

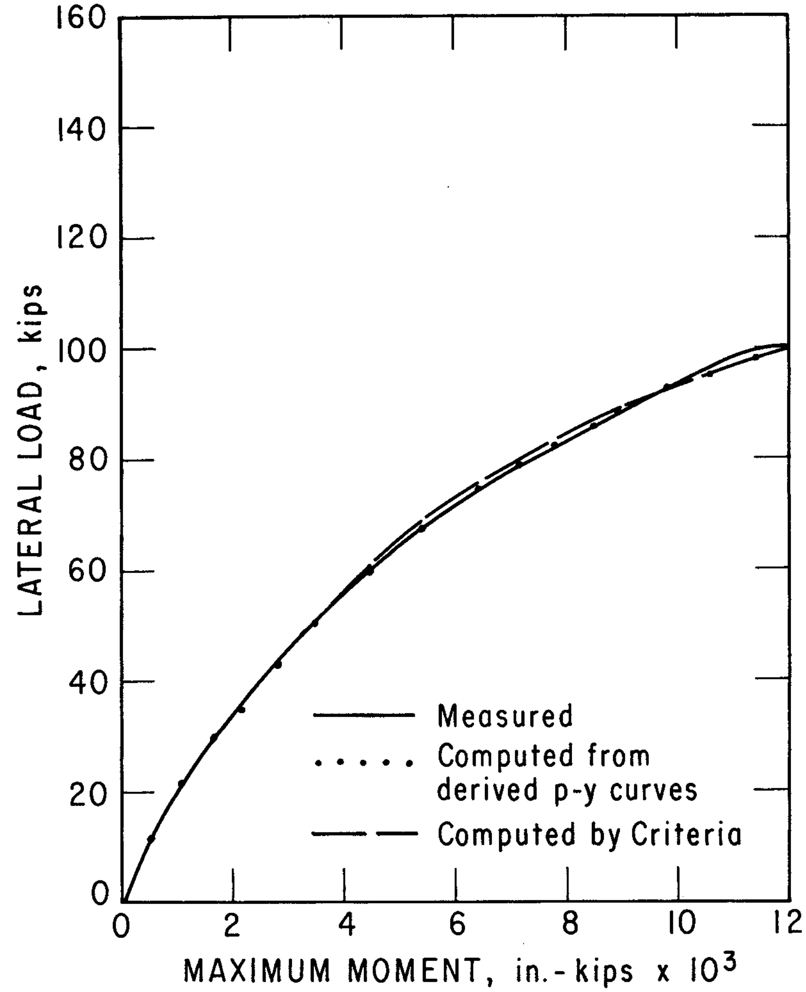

Fig. 24 - Comparison between measured and computed values of maximum bending moment for cyclic loading, 24-in diameter pile. (Pile 2).

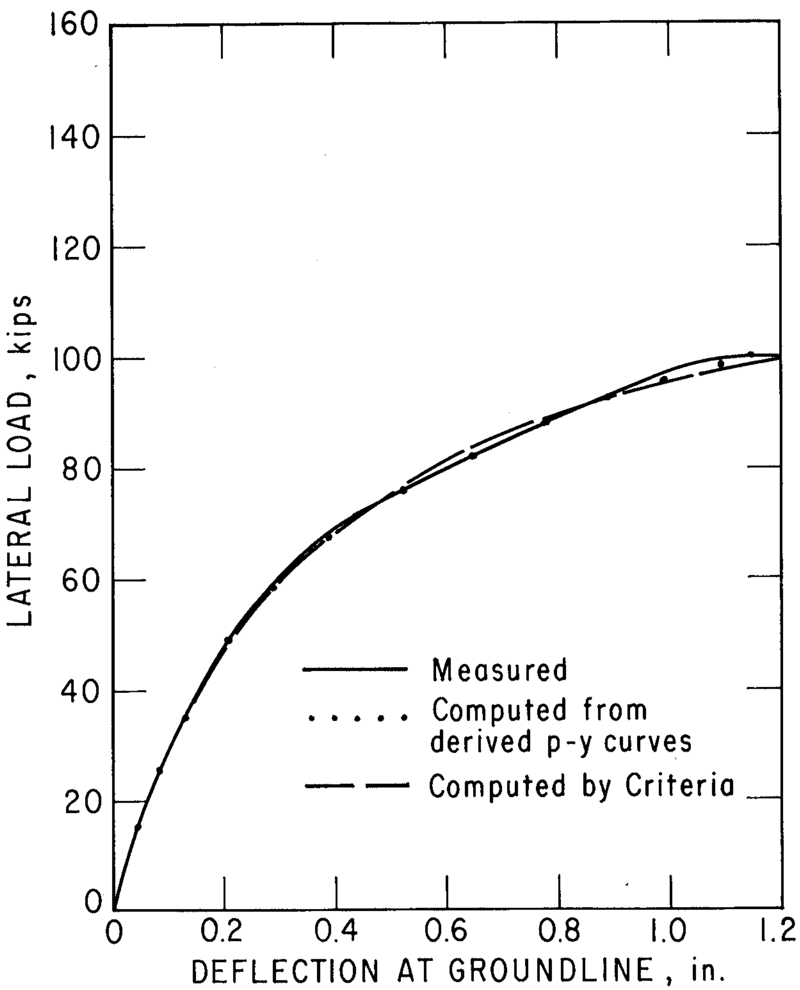

Fig. 25 - Comparison between measured and computed values of de lection at groundline for cyclic loading, 24-in diameter pile. (Pile 2).

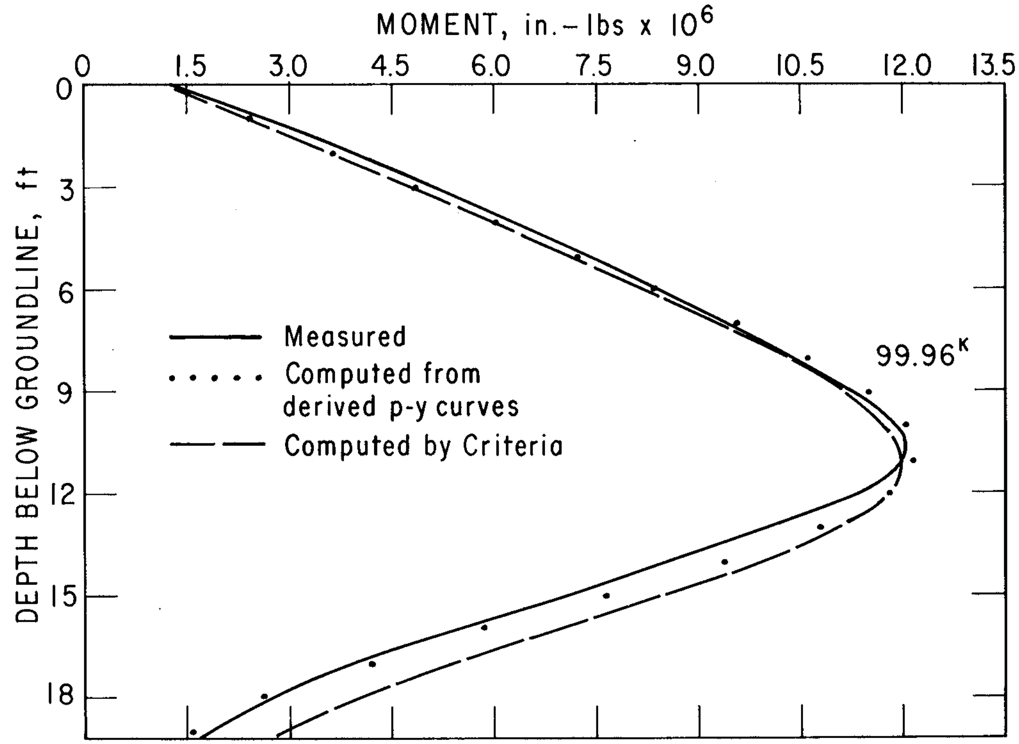

Fig. 26 - Comparison between measured and computed bending moment curves for cyclic loading and for maximum lateral load, 24-in diameter pile. (Pile 2).